

# A Contribution to Time-Dependent Damage Modeling of Composite Structures

Paul Treasurer, Yann Poirette, Dominique Perreux, Frédéric Thiebaud

► **To cite this version:**

Paul Treasurer, Yann Poirette, Dominique Perreux, Frédéric Thiebaud. A Contribution to Time-Dependent Damage Modeling of Composite Structures. Applied Composite Materials, Springer Verlag (Germany), 2014, 21, pp.677 - 688. <10.1007/s10443-013-9364-1>. <hal-01085106>

**HAL Id: hal-01085106**

**<https://hal-ifp.archives-ouvertes.fr/hal-01085106>**

Submitted on 20 Nov 2014

**HAL** is a multi-disciplinary open access archive for the deposit and dissemination of scientific research documents, whether they are published or not. The documents may come from teaching and research institutions in France or abroad, or from public or private research centers.

L'archive ouverte pluridisciplinaire **HAL**, est destinée au dépôt et à la diffusion de documents scientifiques de niveau recherche, publiés ou non, émanant des établissements d'enseignement et de recherche français ou étrangers, des laboratoires publics ou privés.

# **A contribution to time-dependent damage modeling of composite structures**

**Paul Treasurer<sup>1,2</sup>, Yann Poirette\*<sup>1</sup>, Dominique Perreux<sup>2,3</sup>, Frédéric Thiebaud<sup>2,3</sup>**

1 - IFP Energies nouvelles, Rond-point de l'échangeur de Solaize, BP 3, 69360 Solaize,  
France

2 - Université de Franche-Comté, LMARC/FEMTO-ST, 24 rue de l'Épitaphe 25000  
Besançon-France

3 - MaHyTec Ltd, 210 Avenue de Verdun, 39100 Dole, France

\*Corresponding author:

[yann.poirette@ifpen.fr](mailto:yann.poirette@ifpen.fr), Tel: 00 33(0)4 37 70 26 64

## **Abstract**

The paper presents a new damage model for predicting stiffness loss due to creep loading and cyclic fatigue. The model, developed within a continuum damage mechanics framework, is based on the idea of a time-dependent damage spectrum, some elements of which occur rapidly and others slowly. The use of this spectrum allows a single damage kinematic to model creep and fatigue damage and to take into account the effect of stress amplitude, R ratio, and frequency. The evolution equations are based on similar equation than the one describing the viscoelasticity model and are relatively easy to implement. The new model is compared to the experimental results on carbon fiber/epoxy tubes. Quasi-static, creep and fatigue tests are performed on filament-wound tubular specimens to characterize the elastic, viscoelastic and plastic behavior of the composite

material. Varying amounts of damage are observed and discussed depending on stress level and R ratio. The experimental work aims to develop and validate the damage model for predicting stiffness loss due to creep loading and cyclic fatigue.

**Keywords:** Fatigue; Creep; Damage mechanics; Modeling

## **1. Introduction**

Composite materials are increasingly being considered for utilization in the petroleum industry [1-3]. Among the possibilities currently being studied is the use of composite materials for the production riser on top-tensioned offshore oil platforms. Currently, production risers are made out of steel; however, as the demand for oil pushes offshore operations into greater depths, the weight of steel risers will become problematic and economically costly. Salama [4] has shown that at depths of 2000 m, the cost of a composite riser becomes comparable to that of a steel riser, and beyond depths of 3000 m composite risers would be considerably cheaper.

Implementing composite materials for this sort of application is not without difficulties, however. Risers are installed for the life of the platform, which can be 20 years or longer. They are subjected to thermomechanical fatigue loads due to waves and tides, constant elevated internal pressures for production, external pressure due to the sea and gradient of temperature mostly between the inner and the external diameter. A good understanding of the behaviour of tubular composite structures subjected to creep and fatigue loading is essential.

The fatigue of composite materials has received a considerable amount of attention over the past decades. Experimentally, the effects of R ratio and frequency have been documented, and the overall damage mechanisms are fairly well understood [5-12]. However, modeling these phenomena remains difficult. A review of existing fatigue models by Degriek and Van Paepegem [7] details the various approaches currently available as well as the difficulties associated with taking into account the experimentally-observed phenomenon.

Some of the difficulty comes from the inability of most existing models to take into account creep-fatigue interaction [7]. Recent works have been devoted to fatigue and creep [11], but the coupling of both phenomena and resulting damage are still an issue. From a practical standpoint this is problematic as some structures experience mixed fatigue-creep loadings requiring different modeling approaches. From a theoretical standpoint, a fatigue damage model should be as accurate for a frequency of 1 Hz as it is at 0.001 Hz, that is to say, as it approaches a creep test. Otherwise, the ability to predict the material response at other frequencies is called into question.

Some approach propose a damaged ply model using an equivalent undamaged ply with an apparent compliance, which is determined as a function of time dependent transverse crack density [13].

One possible approach for addressing these issues is the introduction of a time-dependent damage driving force. A time-independent damage driving force, typically denoted  $Y$ , is used by a number of researchers in determining damage due to quasi-static loadings using a micro-meso model [14-16] or meso-macro model [17-18]. The first models consider the different damage mechanisms and describe their potential synergic effect, typically the diffuse damage (fiber-matrix debonding) and the transverse microcracking [15] while the second ones focus on the matrix cracking and delamination.

In a same thermodynamics framework, a time-dependent damage driving force would perform the same function for cyclic and creep loads. The model presented in this paper proposes an expression for a time-dependent damage driving force easy to identify and implement. It is developed and validated using experimental results of creep and fatigue tests on tubular composite specimens.

## **2. Material**

The material used in this work is a M10 amine/epoxy resin system reinforced by Toray T700S carbon fibres. Tubes with a nominal diameter of 60mm and a 300mm length were manufactured by

Mahytec Company using filament winding process, and then cured according to manufacturer's specifications (curing temperature of 120°C for four hours). The use of tubular specimens rather than flat specimens was justified by the lack of edge effects results in a more uniform stress state, as well as the fact that the targeted industrial application in this study is a tubular structure. Six lay-ups were considered in this study.  $[\pm 15^\circ]$ ,  $[\pm 45^\circ]$ , and  $[\pm 75^\circ]$  laminates were tested in order to identify the longitudinal, shear and transverse behaviours of the composite material. Additionally,  $[\pm 55^\circ]$ ,  $[\pm 60^\circ]$  and a proprietary  $[\pm\theta/\pm\phi]$  (where  $\theta$  is a winding angle for circumferential rigidity and  $\phi$  a winding angle for axial rigidity) were tested for model validation. The nominal thickness of the specimens is 1.2 mm except for the  $[\pm\theta/\pm\phi]$  lay-ups which have a thickness of 2.4 mm. For each laminate, quasi-static, creep, and fatigue tests were performed. Quasi-static and creep tests were used to characterise the elastic, plastic and visco elasto plastic behaviour of the material [23].

### 3. Quasi-static Damage Model

The model, firstly developed by Thiebaud and Perreux [18] and extended latter to the mesoscopic scale by Perreux and Lazuardi [22], is the basis of the new time-dependent damage model proposed in the following section. This model is based on Continuum Damage Mechanics, using the internal state variables  $D_i$  to describe the stiffness loss due to microcracking. The stiffness loss is taken into account using a damaged compliance tensor given as

$$\tilde{\mathbf{S}} = \mathbf{S} + \mathbf{H} \quad (1)$$

$$\text{where } \mathbf{H} = \begin{bmatrix} 0 & 0 & 0 \\ 0 & H_{22} & 0 \\ 0 & 0 & H_{66} \end{bmatrix}$$

The damage variables  $D_I$  and  $D_{II}$  are written as

$$D_I = -\frac{\Delta E_2}{E_2} = 1 - \frac{S_{22}}{S_{22} + H_{22}} \quad (2)$$

$$D_{II} = -\frac{\Delta G_{12}}{G_{12}} = 1 - \frac{S_{66}}{S_{66} + H_{66}}$$

These damage variables are linked to the density of microcracks [19] and could be expressed from each other::

$$D_{II} = 1 - S_{66} \left[ S_{66} + \frac{D_I}{(1 - D_I)^{1/2}} (S_{11} S_{22})^{1/2} \right]^{-1} \quad (3)$$

Thus, only  $D_I$  is necessary to describe the effect of microcracks on the transverse and shear moduli. In order to determine the evolution of  $D_I$ , an associated plasticity formalism with the following damage criterion is used:

$$f^D = -Y - R^D - Y_C \leq 0 \quad (4)$$

where  $Y$  is the damage motor force,  $Y_C$  is the damage yield point for the ply, and  $R^D$  represents the accumulated damage. Damage occurs when the two following conditions are fulfilled:

$$f^D = 0 \text{ and } \frac{\partial f^D}{\partial Y} \dot{Y} > 0$$

The form of the hardening function  $R^D$  is chosen so as to provide coherence with experimental observations. A power law is proposed:

$$R^D = \alpha (D_I)^P \quad (5)$$

where  $\alpha$  and  $P$  are material parameters.

The damage driving force  $Y$  is defined as the partial derivative of the free energy density  $\psi$  with respect to damage  $D_I$ :

$$Y = \frac{\partial \psi}{\partial D_I} \quad (6)$$

$$\text{where } \psi = \frac{1}{2} \boldsymbol{\varepsilon}^e : \tilde{\mathbf{S}}^{-1} : \boldsymbol{\varepsilon}^e + \psi^* \quad (7)$$

where  $\psi^*$  is a function of other internal variables.

The evolution of damage and its effect on the elastic behavior of the lamina can now be determined using the relation

$$\dot{D}_I = -\lambda^D \frac{\partial f^D}{\partial Y} \quad (8)$$

where  $\lambda^D$  is the Lagrange multiplier.

#### 4. Development of Time-Dependent Damage Model

The above formulation is valid only for the first cycle of a fatigue test or the initial loading of a creep test. In order to include any subsequent creep or fatigue damage, an additional damage kinematic taking into account the time dependant phenomenon is needed.

Joseph and Perreux [17], for example, proposed the following damage evolution law:

$$\dot{D}_I = -\lambda^D \frac{\partial f^D}{\partial Y} - \frac{\partial \varphi^*}{\partial Y} \quad (9)$$

where  $Y$  is the static damage driving force,  $f^D$  is a static damage criteria,  $\lambda^D$  a Lagrange multiplier, and  $\varphi$  is a dissipation potential defined as:

$$\varphi^* = \frac{K_D}{(n_D + 1)(D_c - D_I)^2} \left\langle \left[ -Y - R^D + g(D_I) \right] (D_c - D_I)^2 - Z - Y_C \right\rangle^{n_d + 1} \quad (10)$$

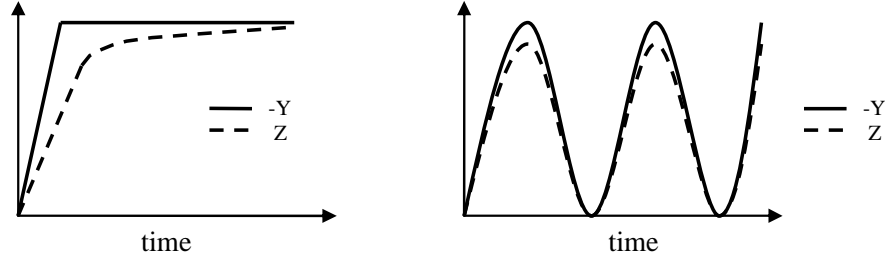
where  $K_D$ ,  $n_D$ ,  $D_C$ , and  $Y_C$  are model parameters,  $R^D$  takes into account accumulated damage, and the variable  $Z$  is the time-dependent damage driving force which essentially lags behind  $Y$  as shown in

Fig. 1.  $Z$  is defined with the following equations :

$$Y(D_C - D_I)^2 < Y_C \quad \rightarrow \quad \dot{Z} = 0$$

$$Y(D_c - D_l)^2 < Z + Y_c \quad \rightarrow \quad \dot{Z} = \frac{1}{\tau_1} \{Y(D_c - D_l)^2 - Z - Y_c\} - \frac{1}{\tau_2} Z$$

$$Y(D_c - D_l)^2 = Z + Y_c \text{ and } \dot{Y} < 0 \quad \rightarrow \quad \dot{Z} = Y(D_c - D_l)^2$$



**Fig. 1** Role of Z in creep and fatigue modeling

While initial results of this approach showed promise for taking into account the effects of frequency, average stress, stress amplitude and creep damage, in practice this approach proved too complicated to implement because of the complexity involved in determining Z. Nevertheless, this approach is conceptually satisfying, and so the present work will seek to propose a simpler model while keeping several aspects of the aforementioned model.

The new damage model is based on the idea of a damage spectrum, which assumes that the time-dependent propagation of a microcrack will be influenced by several factors, such as the orientation of the polymer chains that must be broken for the crack to propagate, proximity to fibers, and proximity to other microcracks or voids. The rate of loading and time under load will determine which phenomena are activated. The net result is that some cracks propagate rapidly and others slowly, and the overall damage is the sum of a spectrum of damages.

The rate of change of the damage is the sum of the rate of change of the instantaneous damage as defined in equation (8), and the rate of change of a time-dependent damage  $\dot{D}_l^*$ :

$$\dot{D}_l = -\lambda^D \frac{\partial f^D}{\partial Y} + \dot{D}_l^* \quad (11)$$



where  $\dot{D}_I^*$  is the sum of the elementary time-dependent damages:

$$\dot{D}_I^* = \sum_i \dot{d}_{I,i} \quad (12)$$

Each elementary damage  $d_{I,i}$  will be driven by an associated variable  $y_i$ . As in equation (6), this is written:

$$y_i = -\frac{\partial \psi}{\partial d_{I,i}} \quad (13)$$

This formulation is inspired by the viscoelastic model, proposed by Petipas *et al.* [20], also based on a spectrum. In this approach, a family of second-order tensors  $\xi_i$ , corresponding to the mechanisms of viscoelastic flow, are defined. Each  $\xi_i$ , with driving force  $\chi_i$ , is associated with a relaxation time  $\tau_i$  and weighted by  $\mu_i$ ; the weighted sum of these elementary strains gives the overall viscoelastic strain. The free energy density is written as:

$$\psi = \frac{1}{2} \boldsymbol{\varepsilon}^e : \mathbf{C} : \boldsymbol{\varepsilon}^e + \frac{1}{2} \sum_i \frac{1}{\mu_i} (\xi_i : \mathbf{C}_R : \xi_i) + \psi^* \quad (14)$$

where  $\boldsymbol{\varepsilon}^e$  is the elastic strain and  $\mathbf{C}$  and  $\mathbf{C}_R$  are respectively the elastic and viscoelastic stiffness matrices, given by:

$$\mathbf{C} = \mathbf{S}^{-1} = \begin{bmatrix} S_{11} & S_{12} & 0 \\ S_{12} & S_{22} & 0 \\ 0 & 0 & S_{66} \end{bmatrix}^{-1}, \quad \mathbf{C}_R = \mathbf{S}_R^{-1} = \begin{bmatrix} 0 & 0 & 0 \\ 0 & \beta_{22} S_{22} & 0 \\ 0 & 0 & \beta_{66} S_{66} \end{bmatrix}^{-1} \quad (15)$$

The associated driving force  $\chi_i$  is obtained from (14):

$$\chi_i = \frac{\partial \psi}{\partial \xi_i} \quad (16)$$

Using a similar formalism, the evolution of the damage  $y_i$  will be determined by a potential  $\varphi$ .

Based on experimental observations, the following form is proposed:

$$\varphi = -\frac{1}{2} \sum_i \frac{\mu_i}{\tau_i} (1 - D_I)^\alpha \beta (-Y + y_i)^2 \quad (17)$$

Here  $\mu_i$  and  $\tau_i$  define the damage spectrum, which is chosen as triangular (Fig. 2) as suggested by Richard and Perreux [21] for ease of implementation, and is found from the equations:

$$\tau_i = 10^{n(i)}$$

$$\begin{aligned} \mu_i &= +a[n(i) - (n_c - n_0)] && \text{for } n(i) \in [(n_c - n_0), n_c] \\ \mu_i &= -a[n(i) - (n_c + n_0)] && \text{for } n(i) \in [n_c, (n_c + n_0)] \end{aligned}$$

$$\text{where } a = \frac{2}{n_0(n_b - 1)}$$

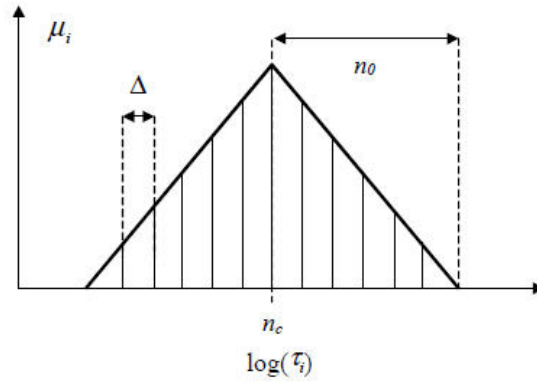


**Fig. 2** Relaxation time spectrum

Additionally, the spectrum is normalized so that

$$\sum_{i=1}^{n_b} \mu_i = 1$$

Finally, the rate of change of each  $d_i$  is obtained from the derivative of the potential with respect to

$y_i$ :

$$\dot{d}_i = -\frac{\partial \varphi}{\partial y_i} = \frac{\mu_i}{\tau_i} (1 - D_I)^\alpha \beta (-Y + y_i) \quad (18)$$

The formulation up to this point can be used to describe the initial stiffness loss and subsequent stabilization; in order to predict the acceleration of damage prior to final failure, an additional relation is needed. While predicting the fatigue life of a structure is complicated, and the material behavior model developed here is not strictly speaking adequate for predicting failure, an attempt can be made at simulating the final portion of life. The braking parameter can be taken as constant until a critical amount of damage is reached, when damage accelerates and macrocracking, delamination, and other structural effects become more important. At this point a linear degradation of the braking parameter is proposed, resulting in an acceleration of  $D_I$ :

$$\begin{cases} D_I < D_{crit} & \Rightarrow & \alpha = \alpha_{ini} \\ D_I \geq D_{crit} & \Rightarrow & \alpha = \frac{1 - \alpha_{ini}}{1 - D_{crit}} D_I + \frac{\alpha_{ini} - D_{crit}}{1 - D_{crit}} \end{cases} \quad (19)$$

This is shown schematically in Fig. 3.

The critical damage parameter  $D_{crit}$  does not appear in any other equation or calculation, and is not integral to the model. It can thus be omitted if the final stages of damage evolution are not needed.

In order to determine the structural response of the laminate, an approach based on classical lamination theory extended for non-linear responses is used [22]. This approach consists of writing solving the generalized forces and moments for incremental strains and curvatures using the tangential matrices - not the traditional elastic  $\mathbf{A}$ ,  $\mathbf{B}$  and  $\mathbf{D}$  matrices.

$$\begin{pmatrix} \Delta \mathbf{N} \\ \Delta \mathbf{M} \end{pmatrix} = \begin{bmatrix} \mathbf{A}^* & \mathbf{B}^* \\ \mathbf{B}^* & \mathbf{D}^* \end{bmatrix} \begin{pmatrix} \Delta \boldsymbol{\varepsilon}_0 \\ \Delta \boldsymbol{\rho} \end{pmatrix} \quad (20)$$

Equations (19) and (20) determine the fatigue and time-dependent damage of a laminate.

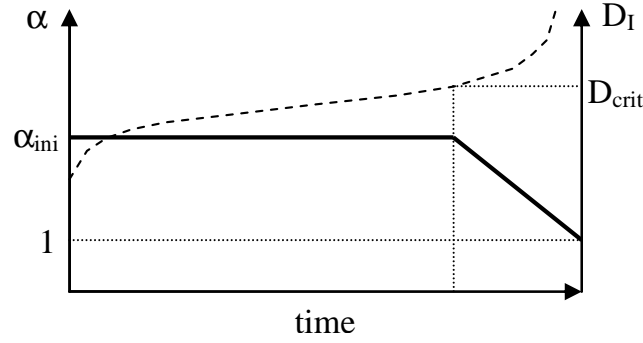


**Fig. 3** Evolution of parameter  $\alpha$  with damage

#### 4.1 Role of Model Parameters

In the above formulation, there are a total of 4 parameters. The relaxation times  $\tau_i$  and associated weights  $\mu_i$  are the same as those used in viscoelastic modeling; these can be identified with a traditional creep test [23]. Parameter  $\beta$  determines the magnitude of damage possible for a given stress state, and is largely analogous to the matrix  $\mathbf{S}_R$  in viscoelasticity. This parameter is scaled by  $(1 - \bar{D}_I)^\alpha$  to take into account the change in damage propagation with accumulated damage, which generally occurs more rapidly at the beginning of a test and then slows; parameter  $\alpha_I$  determines the extent of this "braking" phenomena. Finally, in equation (18) the  $y_i$  lag behind the instantaneous force  $Y$ , and this difference is what drives the time-dependent damage development.

As shown experimentally, the damage tends towards a certain characteristic damage state (CDS), and, the parameter  $\beta$  will be used to ensure consistence with this state for any set of parameters. In other words, once a potential set of parameters is identified, an optimization of the parameter  $\beta$  is performed. Thus, any change in  $\alpha$ ,  $n_c$ , and  $n_0$  requires a modification of  $\beta$  to assure that the experimentally-observed CDS is maintained. This step is relatively quick, as each simulation takes approximately one minute. However, its identification, and thus the experimental determination of the characteristic damage state via a creep test, is indispensable to the model.

The parameter  $\alpha$  determines the influence of accumulated damage on damage progression. A value of between 2.0 and 3.0 appears necessary to describe the generally observed pattern of a rapid loss of stiffness followed by a stabilization.

The choice of the  $n_c$  and in  $n_0$  is clearly a fundamental aspect of this modeling approach. As  $n_c$  increases, the rate of damage progression slows. As  $n_c$  represents the centre point of the spectrum, this is not surprising: essentially, more time is needed for damage phenomenon to manifest.

Similarly, as  $n_0$  increases, the rate of damage progression increases. By increasing the width of the spectrum, a higher weight is assigned to earlier phenomenon, thus increasing the speed at which damage occurs. This also determines the effect of frequency on damage progression: for a given  $n_c$ , a larger value of  $n_0$  will cause a greater rate of damage than a smaller value of  $n_0$ .

The role of the parameters now being understood, it is possible to identify them for an actual material system.

#### **4.2 Method of parameters identification**

As previously discussed, fatigue, creep, and their interaction with each other influence fatigue life. As such, two different fatigue tests at 65 MPa and 85 MPa with different R ratios (0.1 and 0.3 respectively) and a creep test at 85MPa on [ $\pm 45^\circ$ ] tubes are used for the identification process. The identification is made from the measurement of the damage frequently characterized by the stiffness loss [7, 24]. During creep tests or cyclic tests, after loading to a certain stress level or after a certain number of cycles respectively, the specimen was unloaded and the variation in the axial modulus was measured:

$$D_{zz} = \Delta E_{zz} / E_{zz}$$

The process of identification used is an iterative one. An initial choice of  $\alpha$  is made based on the overall trends observed in the fatigue tests; this value will be fixed during identification of parameters  $n_c$  and  $n_0$ , although it is possible to refine this choice later. Here,  $\alpha=2.5$  is selected. The values of  $n_c$  and  $n_0$  are systematically varied by a certain percentage, for example 5% or 10%; for each variation,  $\beta$  is determined. The fatigue tests are simulated and the residual, based on the error between the simulation and the experimental results, is evaluated; based on the best result, a new  $n_c$  and  $n_0$  are determined. This iterative process is repeated until a satisfactory fit is obtained for the fatigue tests. As it can be time consuming to simulate each fatigue test to failure (approximately 120 to 140 cycles per minute), it is more practical to optimize the parameters based on the damage level at a relatively early stage in the test. As such the optimization is only performed on the results of the first 5000 cycles of the test.

The parameters are determined using an iterative process. The identified values are reported in Table 1.

**Table 1.** Identified value of parameter

Parameter	Value
$\beta$	350
$\alpha$	2.5
$n_c$	5.00
$n_0$	3.25

## 5. Comparison of model with creep and fatigue tests

The parameters being identified, it is now possible to validate the model against other loadings and lay-ups. In Fig. 4, the model is compared with the results of the fatigue tests performed at  $f=2$  Hz on the  $[\pm 45^\circ]$  lay-up. Due to time computation, the simulations are made on relatively low number of cycles. It is recalled that only the first 5000 cycles of the tests at  $\sigma_{\max}=85$  MPa with  $R=0.3$  and

$\sigma_{\max}=65$  MPa and  $R=0.1$  were used for the identification. Given the dispersion inherent in fatigue testing, a good correlation is found (Fig. 4). The difference between  $\sigma_{\max}=85$  MPa and  $\sigma_{\max}=65$  MPa is predicted, as well as the difference in R ratios at both stress levels.

Using the same set of parameters, the creep damage evolution can be predicted (Fig. 5). While it is not a surprise that the final value of  $D_{zz}$  corresponds to the data as it was used for the optimization, it should be noted that the form of the curve, which is determined by  $n_c$ ,  $n_0$ , and  $\alpha$ , also correlates well with the experimentally observed evolution. This gives some credibility to the notion of a single damage spectrum which determines the overall fatigue and creep damage behavior of a material.

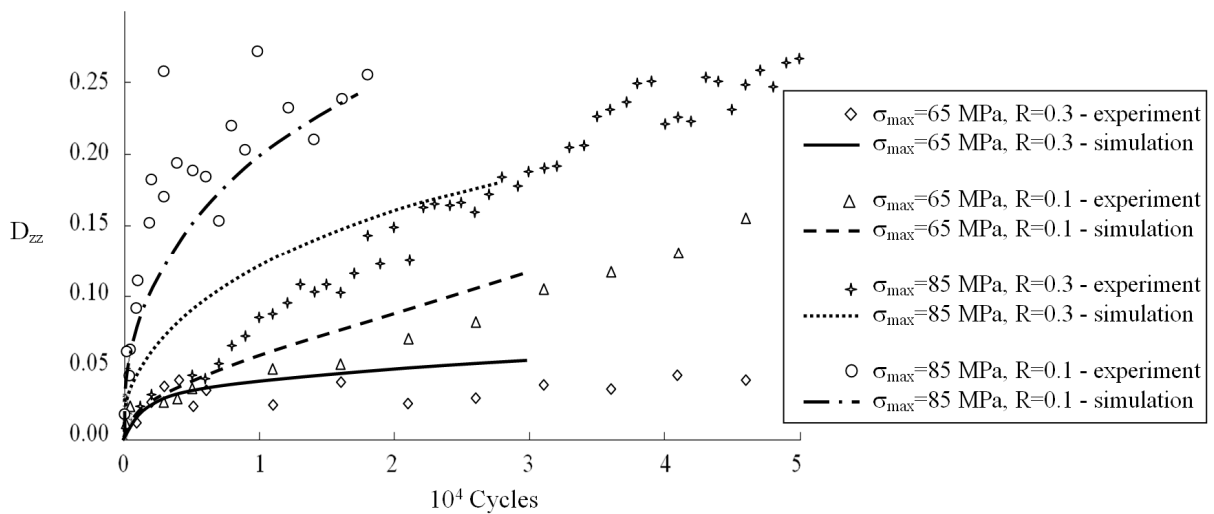


**Fig. 4** Comparison of damage evolutions resulting from the model and fatigue tests at different loadings on  $[\pm 45^\circ]$  lay-up ( $f=2$  Hz)

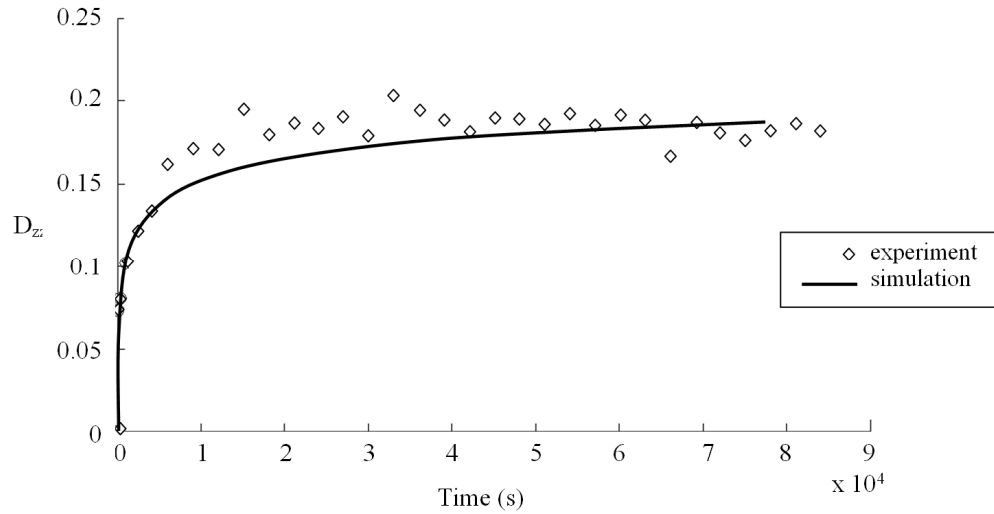


**Fig. 5** Comparison of the damage evolution resulting from the model and creep test (85 MPa) on  $[\pm 45^\circ]$  lay-up

The model is compared with the test performed at  $f=0.5$  Hz, 2 Hz and 4 Hz in Fig. 6. Given the limited amount of data for  $f=0.5$  Hz and  $f=4$  Hz and experimental variation, the model seems capable of simulating the fatigue-creep interaction effect. The damage evolution at  $f=0.5$  Hz is more rapid than the evolution at 2 Hz, and the progression at 4 Hz is slower than that at 2 Hz. It should be noted that temperature effects would not be predicted with this model, so high frequency tests could only be simulated in an environment where specimen temperature did not exceed a certain level.

A comparison with fatigue data from the  $[\pm\theta/\pm\phi]$  lay-up is shown in Fig. 7. The model is better at predicting high cycle fatigue than predicting low-cycle fatigue. The model also predicts a stabilization in damage progression that does not occur in the test at  $\sigma_{\max}=300$  MPa. This could be due to the braking parameter being load or lay-up dependent.

There is another possible explanation. The damage levels observed experimentally, 0.13 – 0.18, cannot be entirely explained by stiffness loss in the  $\pm\theta$  plies, as elevated damage levels in these plies would result in approximately  $D_{zz}=0.07$ . There is the possibility of propagation of damage



from the  $\pm\theta$  to the  $\pm\phi$  plies, even though damage would not normally occur there. This would result in the additional stiffness loss, although predicting this phenomenon would be extremely difficult.

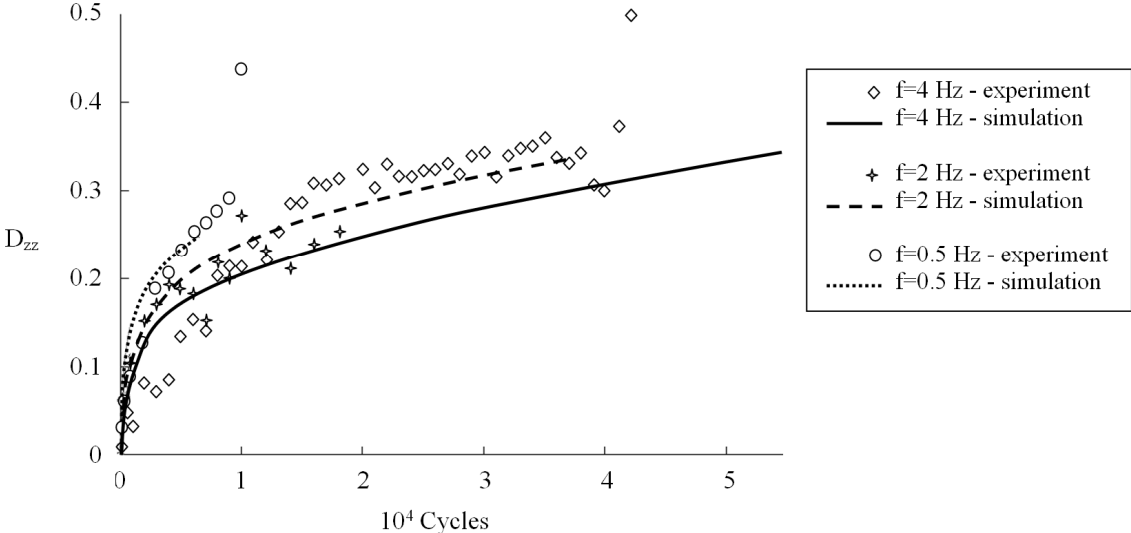


**Fig. 6** Comparison of damage evolutions resulting from the model and fatigue tests -  $\sigma_{\max}=85$  MPa,  $R=0.1$  - at different frequencies on  $[\pm 45^\circ]$  lay-up

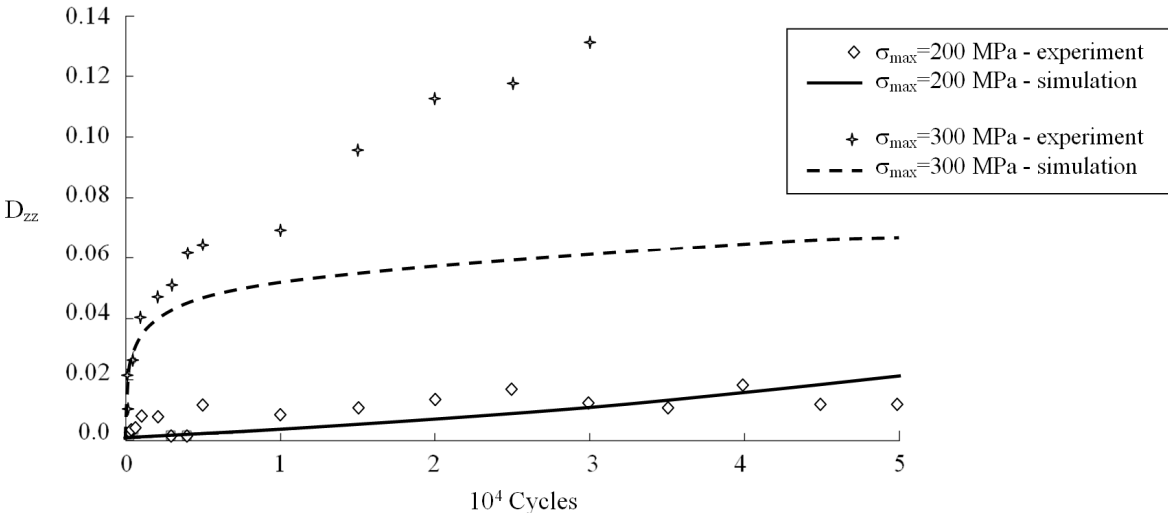


**Fig. 7** Comparison of the damage evolution resulting from the model and fatigue tests at different loadings -  $R=0.1$ ,  $f=2$  Hz - on  $[\pm\theta/\pm\phi]$  lay-up

## **6. Conclusion**

In this paper, a new viscous damage model was developed. It is based on a spectral distribution of time-dependent damage mechanisms, which are then predicted using a dissipation potential similar to that used in viscoelastic modeling. This model is based on the observation of creep and fatigue damage showing that the micro cracking growth is affected by the rate of loading. We have assumed that this phenomenon is connected to polymer relaxation of stress and then the damage kinetics could be described by similar equation than the viscoelasticity strain in polymer. The influence of the various model parameters was discussed, and an approach for identifying them given. Following the identification of these parameters for the material system used in the experimental part of this work, a comparison with the creep and fatigue tests was given. The performance of this model is presented and assessed on various stacking sequence. The materials tested are tubes manufacturing by the same process and the same material in order to reduce the variability of the experimental results. The model is able to predict the effects of frequency, R ratio, and stress level. As it has been observed its accuracy seems especially adapted for predicting high cycle fatigue.

## **Reference**

1. Karayaka M. *et al.*: Composite production riser dynamics and its effects on tensioners, stress joints, and size of deep water tension leg platforms. Offshore Technology Conference, Houston, Texas, 1998

2. Odru P., Poirette Y., Saint-Marcoux J.F., Stassen Y.: Composite riser and export line systems for deep offshore applications. 22<sup>nd</sup> International Conference on Offshore Mechanics and Arctic Engineering, Cancun, Mexico, 2003
3. Martin R.: Composite materials: an enabling material for offshore piping systems. Offshore Technology Conference, Houston, Texas, 2013
4. Salama MM *et al.*: Composite Risers Are Ready for Field Applications – Status of Technology, Field Demonstration, and Life Cycle Economics. 13<sup>th</sup> International Deep Offshore Technical Conference (DOT 2001), October 17-19 2001, Rio de Janeiro, Brazil
5. Perreux D., Joseph E.: Effect of frequency on the fatigue performance of filament-wound pipes under biaxial loading: Experimental results and damage model. *Composites Science and Technology* 57(3), 353-364 (1997)
6. Kaynak C., Mat O.: Uniaxial fatigue behavior of filament-wound glass-fiber/epoxy composite tubes. *Composites Science and Technology* 61(13), 1833-1840 (2001).
7. Degrieck J., Van Paepegem W.: Fatigue damage modeling of fibre-reinforced composite materials: Review. *Applied Mechanics Reviews* 54(4), 279-300 (2001)
8. Moore R.H., Dillard R.A.: Time dependent matrix cracking in cross-ply laminates. *Composites Science and Technology* 39, 1-12 (1990)
9. Raghavan J., Meshii M.: Time dependent damage in carbon fiber reinforced polymer composites. *Composites Part A* 27, 1223-1227 (1996)
10. Guedes R.M.: Time-dependent failure criteria for polymer matrix composites: a review. In *Proceedings of International Conference for Composite Materials 17*, Edinburgh, UK, 27-31 July 2009

11. Miranda Guedes R.: Creep and fatigue in polymer matrix composites, Woodhead Publishing (2010)
12. Nikishkov Y., Makeev A., Seon G.: Progressive fatigue damage simulation method for composites. *International Journal of Fatigue*, In Press, Corrected Proof, Available online 21 November 2012
13. Asadi A and Raghavan J.: Influence of time-dependent damage on creep of multidirectional polymer composite laminates. *Composites Part B: Engineering* 42(3), 489-498 (2011)
14. Ladevèze P.: About a damage mechanics approach. In: Baptiste D (ed) *Mechanics and mechanisms of damage in composites and multi-materials*, pp. 119-141. Mechanical Engineering Publications Limited, London (1991)
15. Ladevèze P. and Lubineau G.: On a damage mesomodel for laminates: micro–meso relationships, possibilities and limits. *Composites Science and Technology* 61(15) , 2149–2158 (2001)
16. Vaughan T.J. and McCarthy C.T.: Micromechanical modelling of the transverse damage behaviour in fibre reinforced composites. *Composites Science and Technology* 71(3), 388-396 (2011)
17. Joseph E. and Perreux D.: A model for predicting the fatigue damage of filament wound pipes. In: *Proceedings of DURACOSYS 95*, pp. 91-100. Brussels, Belgium, 16-21 July 1995, .
18. Thiebaud F. and Perreux D.: Overall mechanical behaviour modelling of composite laminate. *European Journal of Mechanics. A. Solids* 15(3), 423-445 (1996)

19. Perreux D. and Oytana C.: Continuum damage mechanics for microcracked composites, *Journal of Composites Engineering* 3, 115-122 (1993)
20. Petipas C., Maire J.F. and Sigety P.: Modélisation viscoélastique du comportement en fluage d'un composite à fibres de carbone et matrice bismaléimide. In: *Proceedings of French National Colloquium on Composite Materials (JNC 11)*, pp. 845-853. Arcachon, France, 18-20 November 1998
21. Richard F. and Perreux D.: The safety-factor calibration of laminates for long-term applications: behavior model and reliability method. *Composites Science and Technology* 61, 2087–2094 (2001)
22. Perreux D. and Lazuardi D.: The effect of residual stress on the non-linear behaviour of composite laminates Part II. Layer, laminate non-linear models and the effect of residual stress on the model parameters, *Composites Science and Technology* 61, 177-190 (2001)
23. Treasurer P.: Durability of Tubular Composite Structures: Fatigue Time Dependent Damage Modelling. PhD Thesis, IFPEN Report (2010)
24. Dyer K.P., Isaac D.H.: Fatigue behaviour of continuous glass fibre reinforced composites. *Composites Part B* 29B, 725–733 (1998)